Optical Absorption and Photoluminescence Studies of Free-Standing Porous Silicon Films with High Porosities

Dongsheng Xu, Guolin Guo,* Linlin Gui,* and Youqi Tang

Institute of Physical Chemistry, Peking University, Beijing 100871, P. R. China

B. R. Zhang and G. G. Qin

Department of Physics, Peking University, Beijing 100871, P. R. China

Received: February 11, 1999; In Final Form: April 29, 1999

We have prepared noncollapsed free-standing porous silicon (PS) films with various porosities even higher than 90% using the electrochemical etching−electropolishing, chemical dissolving, and supercritical drying methods. The result of a study combining optical absorption and photoluminescence (PL) from free-standing PS films with porosities in the range 41−94% is presented. A blue shift of the transmission curves and an increase of the PL intensity with enhancing porosity have been observed. However, no notable blue shift of the PL peak position with increasing porosity has been observed. Furthermore, the square root of the absorption coefficient (α) of the PS samples with high porosities times photon energy ($h\nu$) vs photon energy can no longer be fitted by a linear function. Even for PS films with porosity of 94%, the absorption data do not show that the nanometer Si particles in the PS have a direct energy gap.

I. Introduction

Since the report of strong visible photoluminescence (PL) from porous silicon (PS) in 1990,[1] much progress has been made in PS research.[2,3] However, the origin of the PL is still controversial, and three main types of models have been proposed. (1) Canham[1] suggested that both photoexcitation and radiative recombination of electron−hole pairs occur within nanometer silicon wires in PS, and their energy gaps become larger than that of bulk Si because of the quantum confinement effect. This model will be referred to hereafter as the quantum confinement (QC) model. Koch et al.[4] believe that electron−hole pairs are photoexcited in nanometer silicon particles (NSPs) and radiatively recombined via Si intrinsic surface states (facetting, steps, ridges, and other structural irregularities on NSP surfaces). Both of the above models considered luminescence to be an intrinsic effect of nanometer Si. (2) The luminescence from PS was attributed to some special luminescence materials such as siloxene,[5] SiH_x complexes,[6] polysilane,[7] defects related to oxygen[8,9] or the surface-bound silanone-based oxyhydrides[10−12] rather than an intrinsic property of nanometer Si. (3) Qin and Jia proposed the quantum confinement/luminescence center (QCLC) model[13] for the oxidized PS and NSP embedded silicon oxide films. In this model, photoexcitation of electron−hole pairs occurs in the NSPs, but most of the photoexcitated electrons and holes transfer from the NSPs into the luminescence center (defects or impurities) in the surrounding SiO_x layers or at the interfaces between NSPs and SiO_x and radiatively recombine there. In addition, both photoexcitation and radiative recombination of electron−hole pairs occurring within the SiO_2 layer in PS also exist.[14,15]

Without any influence from the Si substrates, free-standing PS films allow direct comparison of the PL and absorption spectra and thus may supply direct proof of the origin of the PL. The optical absorption and the PL spectra of free-standing PS films with porosities less than 80% have been widely investigated.[16−21] Several authors observed a blue shift of absorption spectra with increasing porosity due to the quantum confinement effect.[16−18] Measurements of the spectral dependence of the absorption in *meso*-PS have shown that it follows the behavior expected for an indirect semiconductor.[16] As for micro-PS, an exponential increase of the absorption coefficient with energy is observed, but the absorption behavior characterizing direct semiconductors has not been observed.[16−19] Contrarily, the temperature dependence relations of the absorption coefficients of micro-PS and of crystalline silicon are the same.[19] Xie[20] observed that the blue shift of the PL peak position coincided with that of the absorption spectra. Kanemitsu[21] reported that there was no clear size dependence of the PL peak energy while an obvious blue shift of optical absorption was observed with a decrease in the average diameter of Si crystallites. Comparison of the PL and absorption spectra of PS samples with porosities in a wide range will be beneficial for clarifying these discrepant results. However, because the skeleton of PS films will be destroyed by huge capillary forces, no free-standing PS films with porosity higher than 80% has been made under natural drying. The supercritical drying process can prevent the formation of the liquid−vapor phase boundary and thereby eliminate the structural collapse caused by capillary forces. This technique had been used successfully to prepare PS with high porosity.[22−24] Recently, Behren et al.[25] reported that the free-standing PS films with porosities as high as 92% had been obtained on moderately doped p-type silicon substrates using the supercritical drying method. Their experiment results demonstrated unambiguously and quantitatively the role of quantum confinement in the optical properties of PS. In this paper, we presented a new way, including electrochemical etching−electropolishing, chemical dissolving, and supercritical

* To whom correspondence should be addressed. E-mail: guogl@csb0.ipc.pku.edu.cn. Fax: 86-10-62751725.

10.1021/jp990519l CCC: $18.00
Published on Web 06/15/1999

drying process, to prepare the noncollapsed free-standing porous silicon (PS) films with porosities as high as 94% from heavily boron-doped p-type silicon. However, no correlation between the PL with optical absorption spectra of PS films with porosities in the range 73−94% was found.

II. Experimental Section

Free-standing PS films with porosity below 80% were formed by anodization of (111)-oriented p-type silicon wafers (0.01−0.015 Ω·cm) in a HF−ethanol solution at constant current density. The current density (between 30 and 130 mA cm^{-2}) and HF concentration (between 20% and 35%) were adjusted in order to obtain the desired porosity. The PS films were then detached from the substrates by electropolishing at a current density of about 500 mA cm^{-2}. Free-standing PS films with porosities higher than 80% were prepared by a four-step process as follows. In the first step, PS layers with a porosity of about 80% and a thickness of about 50 μm were formed in the dark by electrochemical anodization in HF−ethanol solution (40 wt % HF/C_2H_5OH = 1:1) at constant current density (130 mA cm^{-2}). The anodization time was 10 min. In the second step, the PS layers were detached from the substrate by an electropolishing step with a current density of 300 mA cm^{-2}. For high porosity (above 80%), the PS layers were easy to crack during electropolishing. In the third step, to increase the porosities of free-standing PS films, we apply a chemical etching step. Here, we used chemical etching in the same electrolyte for 7−10 h to obtain ultrahighly porosity. Being rinsed two or three times by using ethanol, these films were then kept wet in ethanol and readied for supercritical drying. In the fourth step, we used a supercritical drying process to obtain the dried films. A detailed description of the apparatus and the procedure of supercritical drying is given in ref 23.

The porosities of the samples are obtained using the formula $P = 1 - W/(SL\rho)$, where P stands for the porosity of the sample, W is the weight of the films (determined by gravimetry, sensitivity of 0.01 mg), S is the area of films, L is the thickness of films (given by scanning electron microscopy), and ρ is the density of crystal silicon (2.33 g cm^{-3}). For each sample both transmission and PL measurements were carried out at room temperature. The transmission spectra were performed on an UV−vis−NIR recording spectrophotometer (UV-3100, Shimadzu) from 2000 to 400 nm. The PL spectra of PS films were measured by using 488 nm excitation light from an Ar^+ laser.

III. Results and Discussion

In dealing with the PS films formed by chemicals dissolved in HF solution for 0, 1, 2, 5, 7, and 10 h with the supercritical drying process, we have obtained noncollapsed free-standing PS films with porosities of 79%, 81%, 83%, 89%, 91%, and 94%, whereas the air-dried free-standing PS films are heavily disintegrated into powder. The transmission spectra of PS films with different porosities are shown in Figure 1. For comparison, we also plotted transmission coefficients of free-standing PS films with porosities below 80%. The thicknesses of all of these PS films were in a range 25−50 μm. In this figure, we observed a continuous blue shift of the transmission curves of PS samples with increasing porosity from 41 to 94%. The blue shift of PS films with porosity of 94% had exceeded that of PS films with porosity of 80% made from a p-type substrate.[16] Meanwhile, we also observed an increase in T_0, the transmission at low energy (the plateau region), with increasing porosity. The refractive index, n, can be deduced from $T_0 = 2n/(n^2 + 1)$. The refractive indices 2.81, 1.46, and 1.22 for PS films with

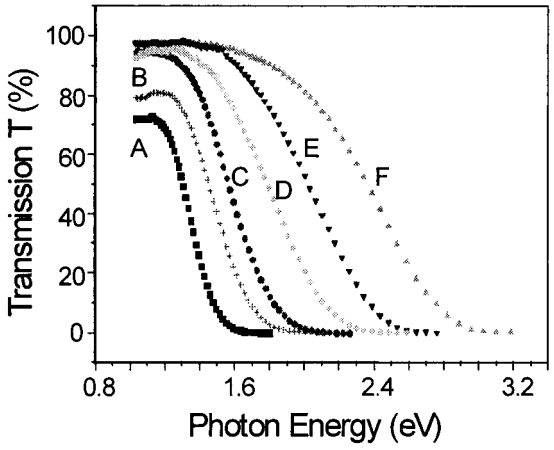

Figure 1. Transmission coefficient vs photon energy for free-standing porous silicon films with porosity of 41% (A), 64% (B), 73% (C), 79% (D), 89% (E), and 94% (F).

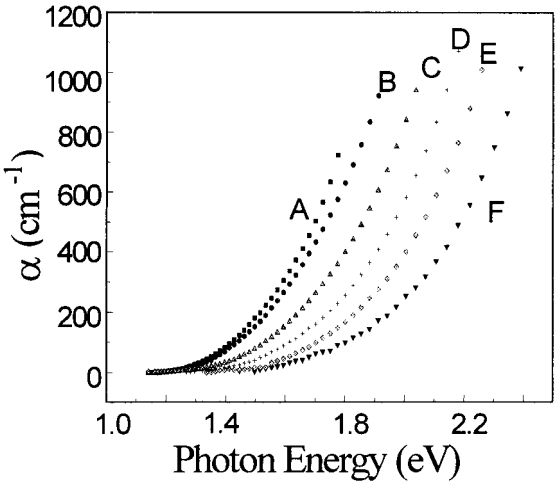

Figure 2. Optical absorption coefficient α vs photon energy for free-standing porous silicon films with porosities of 41% (A), 46% (B), 73% (C), 79% (D), 89% (E), and 94% (F).

porosities of 41%, 79%, and 94% were obtained. The blue shift in the transmission curves and the decrease of the refractive index can be explained by the quantum size effect.[16]

Figure 2 shows the absorption coefficient α versus photon energy of free-standing PS films with different porosities. Similar to ref 16, α is deduced from T using the equation $T = T_0 \exp[-\alpha d(1 - P)]$, where d is the PS layer thickness and $(1 - P)$ is the correction factor for the total quantity of matter. In this figure, a pronounced blue shift of the absorption edge with increasing porosity from 41 to 94% was also observed.

If we take the value of the photon energy where the transmission starts to abruptly decrease, band gaps of 1.15, 1.23, 1.32, 1.43, 1.65, and 1.80 eV can be deduced from the curves A, B, C, D, E, and F in Figure 1, respectively. For PS with a porosity of 41% (curve A in Figure 1), the value of the band gap is very closed to 1.12 eV for c-Si. The blue shift of the absorption edge with porosity was around 280 meV for P = 79% and 650 meV for P = 94% compared to PS films with a porosity of 41%. For PS films with high porosity, especially above 90%, the shift of the absorption edge was already comparable to that of slightly doped PS films with a porosity of about 80%, as reported in ref 16.

Figure 3 shows $(\alpha h\nu)^{1/2}$ versus photon energy $h\nu$ for PS films with porosities of 41%, 79%, and 94%. For the PS films with a porosity of 41%, $(\alpha h\nu)^{1/2}$ is a linear function of photon energy.

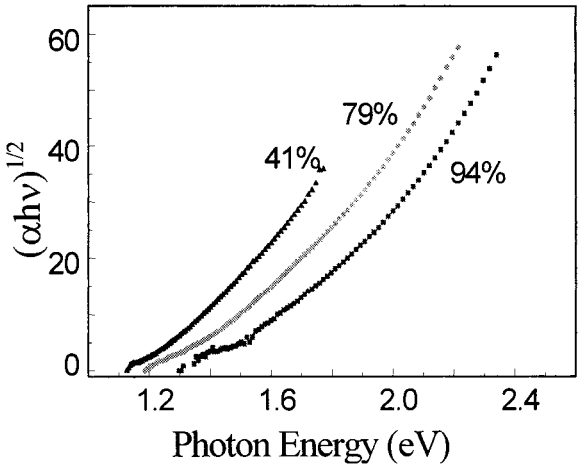

Figure 3. Square root of $\alpha h\nu$ vs photon energy for free-standing porous silicon films with porosities of 46%, 79%, and 94%.

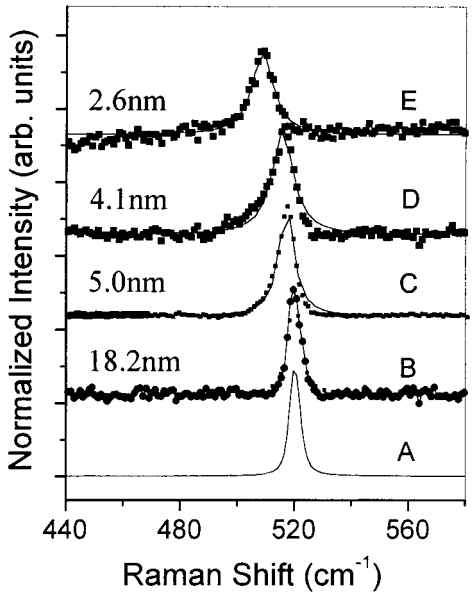

Figure 4. Raman spectra of c-Si (A) and free-standing porous silicon films (full squares) with porosities of 41% (B), 79% (C), 83% (D), and 91% (E). The lines are the theoretical fitting to the experimental data.

An analogous linear function was also observed in films with a porosity below 80%. This result indicates that the absorption for porosity below 80% is very close to that of an indirect band gap semiconductor. However, for porosity above 80%, $(\alpha h\nu)^{1/2}$ can no longer be fitted by a linear function. The absorption data do not show that the nanometer Si particles in the PS have a direct energy gap, even for the PS films with a porosity of 94%.

Figure 4 shows three Raman spectra of c-Si and free-standing PS films with porosities of 41, 79, 83, and 91%. The Raman spectra were shifted to lower energy and broadened with increasing porosity of the PS. A theoretical fit for each experimental curve has been obtained using the model for the Raman line shape,[26,27]

$$I(\omega) = \int_0^1 \frac{\exp[-q^2L^2/(4a^2)]}{[\omega - \omega(q)]^2 + (\Gamma_0/2)^2}\, d^3q$$

where q is expressed in units of $2\pi/\alpha$,α is the lattice constant, and Γ_0 is the line width of the Si LO phonon in c-Si bulk (4.1 cm^{-1} at 520.2 cm^{-1}). We consider the dispersion $\omega(q)$ of the

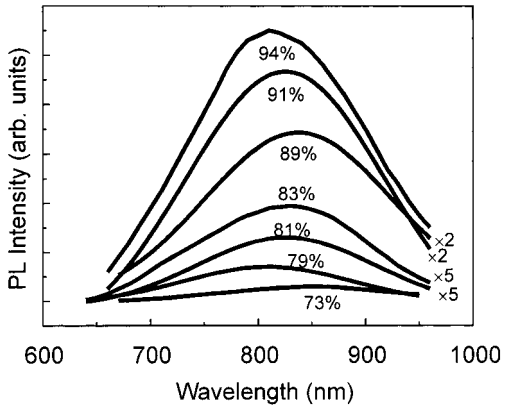

Figure 5. PL spectra from free-standing porous silicon films with porosities of 73%, 79%, 81%, 83%, 89%, 91%, and 94%. The excitation wavelength is 488 nm.

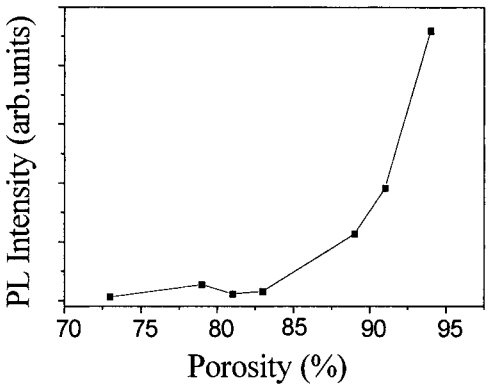

Figure 6. PL intensity vs porosity for free-standing porous Si films.

LO phonon in c-Si to be

$$\omega^2(q) = A + B\cos(\pi q/2)$$

where $A = 1.714 \times 10^5$ cm^{-2} and $B = 1.000 \times 10^5$ cm^{-2}.

The solid lines in Figure 4 are fitting curves, which coincide well with the experimental data. The average diameter (L) of the free-standing PS film with porosities of 41 and 79% is 18.2 and 5.0 nm. After chemical dissolution for 2 and 7 h, the porosities of the PS films with a porosity of 79% have changed to 83% and 91% and the average diameter of the Si crystallites has decreased to 4.1 and 2.6 nm, respectively.

Figure 5 shows the PL spectra of free-standing PS films with various porosities higher than 73% taken at room temperature. No PL of PS films with porosity below 73% was observed. All the PL spectra observed were in the red region or in the near-IR region. Like PS of high porosity adhered on the substrate, the PL intensities of the free-standing PS films with high porosities were also much stronger than those of the PS films with moderate porosities. And the PL intensities of PS films with high porosity sharply increased with increasing porosity [Figure 6]. However, no clear blue shift of the peak maximum position with increasing porosity has been observed, which coincides with other observations on supercritical drying PS.[23,24]

According to the quantum confinement (QC) model of Canham[1] or the Si surface-state model of Koch et al.,[4] the PL peak energies should blue shift with decreasing sizes of the NSPs or increasing band gaps. Distinctly, neither of these models can explain the experimental results presented in this paper. We think that the probable explanation for our experiments is the quantum confinement/luminescence centers model.[13] The QCLC model suggests that the luminescence of PS originates from the

radiative recombination of electron−hole pairs, which are excited in NSPs and then transfer into LCs, at the LCs outside the NSPs units. For as-prepared PS, the main LCs are some absorbates on NSP surfaces. Different fabrication conditions may lead to different density distributions among various absorbates and result in different PL spectra. When oxide layers are grown outside the NSPs, the LCs in SiO_x layers may become the main LCs and thus dominate in luminescence. As we know, all of the PS samples prepared by the supercritical drying process have been slightly oxidized from the results of IR and XPS. Thus, we believe that the PL of free-standing PS films with high porosities also originates from the luminescence centers in Si oxide. The experimental fact for the PL intensity increasing with porosity may be due to a decrease of the nonradiative recombination and an increase of the number of nanometer crystalline Si that can be luminescent. In addition, another probable explanation for these experimental facts is the luminescence centers involving silanone-based silicon oxyhydrides bound to the PS surface.[10−12]

IV. Conclusion

In conclusion, we have prepared the noncollapsed free-standing PS films with various porosities higher than 90% using the electrochemical etching−electropolishing, chemical dissolving, and supercritical drying methods. The optical absorption versus photon energy relation for PS samples with porosities higher than 80% has been studied. A blue shift of the transmission curves and an increase of the PL intensity with enhancing porosity have been observed. For PS films with low porosities, $(\alpha h\nu)^{1/2}$ vs photon energy is nearly a linear function that is similar to what has been observed for an indirect gap semiconductor. For the PS samples with porosities above 80%, $(\alpha h\nu)^{1/2}$ can no longer be fitted by a linear function, but the optical absorption data do not show the characteristic of a direct energy gap even for the PS film with a porosity of 94%. Decreasing the average diameter of the Si crystallites in the PS film with increasing porosity has been obtained by Raman scattering measurements. The PL spectra of PS films with high porosities show that the PL intensity sharply increases with increasing porosity. However, no notable blue shift of the PL peak position with increasing porosity and decreasing size of NSPs has been observed.

Acknowledgment. Project supported by the National Natural Science Foundation of China.

References and Notes

(1) Canham, L. T. *Appl. Phys. Lett.* **1990**, *57*, 1046.
(2) *Porous Silicon*; Feng, Z. C., Tsu, R., Eds.; Word Scientific: Singapore, 1994.
(3) Cullis, A. G.; Canham, L. T.; Calcott, D. J. *J. Appl. Phys.* **1997**, *82*, 909.
(4) Koch, F.; Petrova-Koch, V.; Maschik, T.; Nikolov, A.; Gavrilenko, V. *MRS Symp. Proc.* **1993**, *283*, 197.
(5) Brandt, M. S.; Fuchs, H. D.; Stutzmann, M.; Weber, J.; Cardona, M. *Solid State Commun.* **1992**, *81*, 307.
(6) Tsai, C.; Li, K.-H.; Kinosky, D. S.; Qian, R.-Z.; Tsu, T.-C.; Irby, J. Y.; Banerjee, S. K.; Tasch, A. F.; Campbell, J. C.; Hance, B. K.; White, J. M. *Appl. Phys. Lett.* **1992**, *60*, 1700.
(7) Prokes, S. M.; Glembocki, O. J.; Bermudez, V. M.; Kaplan, R.; Friedersdorf, L.; Searson, P. C. *Phys. Rev. B* **1992**, *45*, 14788.
(8) Prokes, S. M. *Appl. Phys. Lett.* **1993**, *62*, 3244.
(9) Prokes, S. M.; Carlos, W. E. *J. Appl. Phys.* **1995**, *78*, 2671.
(10) Gole, J. L.; Dudel, F. P.; Grantier, D.; Dixon, D. A. *Phys. Rev. B* **1997**, *56*, 2137.
(11) Gole, J. L.; Dixon, D. A. *Phys. Rev. B* **1998**, *57*, 12002.
(12) Gole, J. L.; Prokes, S. M. *Phys. Rev. B* **1998**, *58*, 4761.
(13) Qin, G. G.; Jia, J. Q. *Solid State Commun.* **1993**, *86*, 559.
(14) Qin, G. G.; Lin, J.; Duan, J. Q.; Yao, G. Q. *Appl. Phys. Lett.* **1996**, *69*, 1689.
(15) Qin, G. G.; Liu, X. S.; Ma, S. Y.; Lin, J.; Yao, G. Q.; Lin, X. Y.; Lin, K. X. *Phys. Rev. B* **1997**, *55*, 12876.
(16) Sagnes, I.; Halimaoui, A.; Vincent, G.; Badoz, P. A. *Appl. Phys. Lett.* **1993**, *62*, 1155.
(17) Chan, M. H.; So, S. K.; Cheah, K. W. *J. Appl. Phys.* **1996**, *79*, 3273.
(18) Diligenti, A.; Nannini, A.; Pennelli, G.; Pieri, F. *Appl. Phys. Lett.* **1996**, *68*, 687.
(19) Kovalev, D.; Polisski, G.; Ben-Chorin, M.; Diener, J.; Koch, F. *J. Appl. Phys.* **1996**, *80*, 5987.
(20) Xie, Y. H.; Hybertsen, M. S.; Wilson, William, L.; etc. *Phys. Rev. B* **1994**, *49*, 5386.
(21) Kanemitsu, Y.; Uto, H.; Masumoto, Y.; etc. *Phys. Rev. B* **1993**, *48*, 2827.
(22) Canham, L. T.; Cullis, A. G.; Pickering, C.; Dosser, O. D.; Cox, T. I.; Lynch, T. P. *Nature* **1994**, 368, 133.
(23) Guo, G. L.; Xu, D. S.; Yao, G. Q.; Tang, Y. Q.; Zhang, L. D.; Lin, J.; Ma, S. Y.; Qin, G. G. *Chin. Phys. Lett.* **1996**, *13*, 62.
(24) Frohnhoff, St.; Arens-Fisher, R.; Heinrich, T.; Fricke, J.; Arntzen, M.; Theiss, W. *Thin Solid Films* **1995**, *255*, 115.
(25) von Behren, J.; van Buuren, T.; Zacharias, M.; Chimowitz, E. H.; Fauchet, P. M. *Solid State Commun.* **1998**, *105*, 317.
(26) Richter, H.; Wang, Z. P.; Ley, L. *Solid State Commun.* **1981**, *39*, 625.
(27) Campbell, I. H.; Fauchet, P. M. *Solid State Commun.* **1986**, *58*, 739.